Optimizing Electric Vehicle Charging With Energy Storage in the Electricity Market

Chenrui Jin, *Member, IEEE*, Jian Tang, *Member, IEEE*, and Prasanta Ghosh, *Senior Member, IEEE*

Abstract—The Information and Communication Technologies (ICT) that are currently under development for future smart grid systems can enable load aggregators to have bidirectional communications with both the grid and Electric Vehicles (EVs) to obtain real-time price and load information, and to adjust EV charging schedules in real time. In addition, Energy Storage (ES) can be utilized by the aggregator to mitigate the impact of uncertainty and inaccurate prediction. In this paper, we study a problem of scheduling EV charging with ES from an electricity market perspective with joint consideration for the aggregator energy trading in the day-ahead and real-time markets. We present a Mixed Integer Linear Programming (MILP) model to provide optimal solutions as well as a simple polynomial-time heuristic algorithm based on LP rounding. In addition, we present a communication protocol for interactions among the aggregator, the ES, the power grid, and EVs, and demonstrate how to integrate the proposed scheduling approach in real-time charging operations. Extensive simulation results based on real electricity price and load data have been presented to justify the effectiveness of the proposed approach and to show how several key parameters affect its performance.

Index Terms—Demand response mechanisms, electric vehicle, ICT, smart grid.

NOMENCLATURE:

T	The total number of timeslots.
N	The number of connected EV.
M	The mark-up price ($/kWh).
g_t	The electricity price at timeslot t ($/kWh).
$a_{t,1}$	The regulation-up price at timeslot t ($/kWh).
$a_{t,2}$	The regulation-down price at timeslot t ($/kWh).
$\hat{g}_t$	The balancing electricity price at timeslot t ($/kWh).
$\hat{a}_{t,1}$	The balancing regulation-up price at timeslot t ($/kWh).
$\hat{a}_{t,2}$	The balancing regulation-down price at timeslot t ($/kWh).

l_t	The base load at timeslot t (kW).
P_i	The upper charging rate limit of EV i (kW).
P_i'	The lower charging rate limit of EV i (kW).
$\bar{P}_{i,t}$	The maximum charging rate limit of EV i at timeslot t (kW).
P_c	The upper charging rate limit of ES (kW).
P_c'	The lower charging rate limit of ES (kW).
P_d	The upper discharging rate limit of ES (kW).
P_d'	The lower discharging rate limit of ES (kW).
C_i	The battery capacity of EV i (kWh).
C_e	The battery capacity of ES (kWh).
E_i	The battery charging efficiency of EV i.
E_e	The charging efficiency of ES.
b_i'	The initial SOC (State Of Charge) of EV i.
b_i	The desired SOC of EV i.
X	The upper SOC limit of ES.
X'	The lower SOC limit of ES.
s_i	The starting time of EV i.
f_i	The finishing time of EV i.
b	The initial SOC of ES.
R	The power delivery capacity (kW).
$h_{i,t}$	The connection time of EV i during timeslot t (h).
F	The penalty factor.
U	The number of ES units.
$x_{i,t}$	The SOC of EV i at the beginning of timeslot t.
$x_{e,t}$	The SOC of ES at the beginning of timeslot t.
$p_{i,t}$	The charging rate of EV i at timeslot t (kW).
$e_{i,t}$	The charging energy of EV i at timeslot t (kWh).
$p_{e,t}$	The charging/discharging (positive for charging, negative for discharging) rate of ES at timeslot t (kW).
$z_{c,t}$	The state of charging ES at timeslot t, 1 if charging, 0 otherwise.
$z_{d,t}$	The state of discharging ES at timeslot t, 1 if discharging, 0 otherwise.

$u_{i,t}$	The regulation-up capacity of EV i at timeslot t (kW).
$d_{i,t}$	The regulation-down capacity of EV i at timeslot t (kW).
$m_{i,t}$	The revenue from EV i at timeslot t ($).
e_t	The total charging energy of connected EVs at timeslot t (kWh).
u_t	The total regulation-up capacity at timeslot t (kW).
d_t	The total regulation-down capacity at timeslot t (kW).
m_t	The total revenue at timeslot t ($).

I. Introduction

BEING BOTH economically and environmentally friendly, Electric Vehicles (EVs) are considered as a promising solution to gas shortage and the increase of CO_2, SO_2 and NO_x emissions [13]. EVs can offer many benefits such as lower operational costs, lower gas emissions, and better utilization of renewable energy. Moreover, because of EVs' controllable charging rates [12], [27], when the power grid calls for extra load or additional power supply in case of generation/load imbalance or system emergency, EVs can respond with temporally increased or decreased charging rates. This is referred to as *regulation service* in the electricity market. An EV charging operator can even gain income from the grid by providing regulation services [9], [14]. However, users may be concerned about the relatively high cost of initial investment on EV purchase and unregulated EV charging may cause system overloading or even breakdown in the power grid [5]. To maximize the benefits of using EVs while maintaining a stable grid system, we need regulated and optimized charging control. A load aggregator can act as an interface between users and the grid operator to provide the regulated charging for EVs with joint consideration for benefits of both users and the grid.

Research has been carried out to study how an aggregator should schedule the charging of EVs to maximize its revenue. However, most of previous works didn't fully consider the characteristics of the electricity market. In the whole-sale electricity market, the aggregator needs to predict/estimate the total energy usage on an hourly basis one day ahead based on historical data without having the complete and accurate knowledge of connected EVs of the next day, i.e., their arrival, departure, and energy demand information. Therefore, many uncertainties are involved during the day-ahead electricity market trading and if prediction is not accurate, there may be significant mismatch between the estimated energy usage and the actual energy usage, for which the aggregator needs to compensate in the real-time market by paying penalty fees. In some business models, such as Better Place [1], the aggregator acts as a middleman between EV users and the electricity market but does not have any direct control over EV charging rates. The Information and Communication Technologies (ICT) that are currently under development for future smart grid systems can enable aggregators to have bidirectional communications with both the grid and EVs to obtain real-time price and load information, and to adjust EV charging schedules in real time. In addition, Energy Storage (ES) can be utilized by the aggregator to mitigate the impact of uncertainty and inaccurate prediction of EV charging in real time in case the EV charging rate adjustment is not sufficient. Specifically, when the estimated energy usage is larger than the actual, we can charge ES with the extra energy instead of selling it back to the market, while, when the estimated energy usage is less than the actual, we can charge EVs with energy stored at the ES instead of buying energy from the market at high prices. In this way, the mismatch can be compensated and the aggregator can avoid paying for penalty fees.

In this paper, considering practical day-ahead and real-time electricity market trading, we exploit the benefits of controlling EV charging by presenting a Mixed Integer Linear Programming (MILP) model to provide optimal solutions for a problem of scheduling EV charging with aid of ES in a smart grid system. We also present a simple heuristic algorithm based on Linear Programming (LP) rounding to solve the problem in polynomial time. In addition, we present a communication protocol for interactions among the aggregator, the ES, the power grid, and EVs, and demonstrate how to integrate the proposed scheduling approach in real-time charging operations. Extensive simulation results based on real electricity price and load data have been presented to justify the effectiveness of the proposed approach by comparing it with a baseline method without regulations and to show how several key parameters affect its performance. To the best of our knowledge, we are the first to exploit the benefits that can be brought by optimized EV charging scheduling with ES in the electricity market.

The paper is organized as follows: We discuss related work in Section II and the system model in Section III. We present our MILP model and heuristic algorithm in Section IV as well as the communication protocol in Section V. Simulation results are presented in Section VI. We conclude the paper in Section VII.

II. Related Work

The optimal operation of an aggregator for controlled EV charging has been studied by a few recent works. In [9], Han *et al.* designed an aggregator that makes efficient use of the distributed power of EVs to produce the desired grid-scale power. Both the cost arising from the battery charging and the revenue obtained by providing the regulation service were considered. A dynamic programming algorithm was presented to compute the optimal charging control for EVs. In [22], Sortomme *et al.* presented algorithms to find optimal charging rates with the objective of maximizing the aggregator's profit and in [21], they presented coordinated charging to minimize distribution system loss. The authors of [10] proposed a method for an analytic estimation of the probability distribution of the procured power capacity to obtain an optimal contract size regarding the frequency of regulation. In a recent work [6], the authors presented a new approach to analyze the economic impact of Vehicle-to-Grid (V2G) regulation and performed a case study for Germany using average daily data. In [23], the authors analyzed the economic benefit of ES installations in the New York City region for applications such as energy arbitrage and for regulation

services. The authors of [26] proposed to use the Model Predictive Control (MPC)-based scheduling and operational strategy for a power system with ES to save electricity cost in day-ahead and real-time markets with different levels of price and daily load uncertainties. Korpas *et al.* [15] presented a methodology for the operation of a hybrid plant with wind power and hydrogen storage.

ICT have been studied for efficient energy management in smart grids recently. The authors of [11] considered both the power distribution network and the data communication network and jointly optimized the power and bandwidth resource allocation using different utility functions. In [16], the authors designed experiments to test an intelligent energy management system (iEMS) that acts as a central controller to communicate with EVs using ZigBee. In [20], the authors carried out a sensitivity test on communication reliability and showed the impact of communication failure on EV charging control. Two different V2G communication and control architectures were compared for ancillary services in the US in [19].

The differences between our work and these related works are summarized as follows: 1) Some related works on EV charging [9], [16], [19]–[22] didn't carefully address the characteristics of the day-ahead and real-time electricity markets. 2) How to leverage ES for EV charging is the main focus of this work, which, however, has not been considered by most related works on EV charging [6], [9], [10], [16], [19]–[22]. 3) EV charging has not been considered by related works on utilizing ES for a grid system [15], [23], [26]. 4) The problems considered in [11] are mathematically different from the problem studied here.

III. SYSTEM MODEL

A. Electricity Market Model

There are two kinds of electricity wholesale market settlement approaches: single-settlement and multi-settlement. We focus on the multi-settlement approach since it has been widely adopted by Independent System Operators (ISOs) of power grids. In a multi-settlement system, estimated energy usages are submitted one day ahead from the demand side to the day-ahead market.

In the day-ahead market, the aggregator pays for the estimated energy usage for the next day, as the *first* settlement. The day-ahead electricity price f^{dah} is used in the first settlement, which is given as follows:

$$f^{dah} = \sum_{t=1}^{t=T} \left(g_t^{dah} \sum_{i=1}^{i=N} e_{i,t}^{est} \right); \qquad (1)$$

where T is the number of timeslots and one timeslot has a duration of one hour since both energy trading and scheduling are conducted on an hourly basis; N is the number of EVs connected to the grid; g_t^{dah} is the day-ahead electricity price at timeslot t; $e_{i,t}^{est}$ is the estimated energy usage of EV i at timeslot t. Thus we can have the total estimated energy usage of EVs at timeslot t as $e_t^{est} = \sum_{i=1}^{i=N} e_{i,t}^{est}$.

After the day-ahead market, during the real-time market, the power grid operator may accept energy usage changes up to an hour before real time. Deviations from day-ahead schedules are settled with real-time prices. There may be a penalty for the adjustment of real-time energy usage. The payment in the real-time electricity market is called the *second* settlement electricity cost f^{bal}, which is calculated as follows:

$$f^{bal} = \sum_{t=1}^{t=T} \hat{g}_t^{real} \left(\sum_{i=1}^{i=N} e_{i,t} - e_t^{est} + p_{e,t} \Delta t \right); \qquad (2)$$

where $e_{i,t}$ is the real-time energy usage of EV i at timeslot t. $p_{e,t}$ is the charging rate of ES at timeslot t. Since the duration of one timeslot $\Delta t = 1$, it has the same value as the charging energy of ES at timeslot t. $\hat{g}_t^{real}$ is the real-time balancing price at timeslot t and is given by

$$\hat{g}_t^{real} = \begin{cases} (1+F)g_t^{real}, & \text{if } \sum_{i=1}^{i=N} e_{i,t} - e_t^{est} + p_{e,t} > 0; \\ (1-F)g_t^{real}, & \text{otherwise}; \end{cases} \qquad (3)$$

where g_t^{real} is the real-time electricity price at timeslot t; $e_{i,t}$ is the real-time energy usage of EV i at timeslot t and F is the penalty factor. The total electricity cost is the sum of the first and the second settlement electricity costs $f^{dah} + f^{bal}$. The multi-settlement system gives an aggregator the ability to control energy usage more flexibly.

Regulation service, which is a kind of power system ancillary service provided by aggregators to the power grid, is traded in the ancillary service market, which is very similar to the electricity market, except that the trading price is the regulation service price instead of the electricity price. The regulation revenue of an aggregator in the first settlement v^{dah} is given by the following equation:

$$v^{dah} = \sum_{t=1}^{t=T} \left(a_{t,1}^{dah} \sum_{i=1}^{i=N} u_{i,t}^{est} + a_{t,2}^{dah} \sum_{i=1}^{i=N} d_{i,t}^{est} \right); \qquad (4)$$

where $a_{t,1}^{dah}$ is the day-ahead regulation-up price at timeslot t; $a_{t,2}^{dah}$ is the day-ahead regulation-down price at timeslot t; $u_{i,t}^{est}$ is the estimated regulation-up capacity of EV i at timeslot t and $d_{i,t}^{est}$ is the estimated regulation-down capacity of EV i at timeslot t. The real-time market will settle any mismatch between the estimated regulation service and the actual service. The regulation service revenue at the second settlement v^{bal} is computed as follows:

$$v^{bal} = \sum_{t=1}^{t=T} \left(\hat{a}_{t,1}^{real} \left(\sum_{i=1}^{i=N} u_{i,t} - u_t^{est} \right) + \hat{a}_{t,2}^{real} \left(\sum_{i=1}^{i=N} d_{i,t} - d_t^{est} \right) \right); \qquad (5)$$

where u_t^{est} and d_t^{est} are the total estimated regulation-up and regulation-down capacity respectively. $u_t^{est} = \sum_{i=1}^{i=N} u_{i,t}^{est}$ and $d_t^{est} = \sum_{i=1}^{i=N} d_{i,t}^{est}$.

$$\hat{a}_{t,1}^{real} = \begin{cases} (1+F)a_{t,1}^{real}, & \text{if } \sum_{i=1}^{i=N} u_{i,t} - u_t^{est} < 0; \\ 0, & \text{otherwise}; \end{cases} \qquad (6)$$

$$\hat{a}_{t,2}^{real} = \begin{cases} (1+F)a_{t,2}^{real}, & \text{if } \sum_{i=1}^{i=N} d_{i,t} - d_t^{est} < 0; \\ 0, & \text{otherwise}; \end{cases} \qquad (7)$$

where $a_{t,1}^{real}$ and $a_{t,2}^{real}$ are the real-time regulation-up and regulation-down prices at timeslot t respectively. $u_{i,t}$ and $d_{i,t}$ are the real-time regulation-up and regulation-down capacities of

EV i at timeslot t respectively. The total regulation revenue is the sum of the first and the second settlement regulation revenues $v^{dah} + v^{bal}$.

Each day, before the electricity market closes (usually at 10 A.M. [2]), the load aggragator establishes an estimated schedule of energy usage and regulation capacity for each hour of the next day (which are traded in the day-ahead market [15]) based on electricity prices, base loads (contributed by other electronic appliances), and EV charging demands predicted using historical data.

The aggregator aims to maximize its revenue using an optimized charging control strategy. We consider a general EV charging scenario in which the charging period may span two days, e.g., starts from 12 P.M. of current day and ends at 12 P.M. of the next day. As [2], a forecast of EV charging demands for up to 48 hours is assumed to be available.

Due to unforeseen variations in generation and consumption, and limited power delivery capacity, there may be mismatches between the actual and estimated energy usages. If the real-time energy usage is higher than the estimated energy usage, the aggregator can buy from the real-time market for the shortage or discharge ES to charge EVs (whichever option that can benefit the aggregator better will be chosen); if the real-time energy usage is lower than the estimated energy usage, the aggregator can sell extra energy back to the grid or charge ES. The regulation service follows a similar procedure. Depending on the real-time electricity market conditions, mismatches may result in *balancing costs* in the power system and thereby a penalty for energy usage adjustment. Thus we define a *penalty factor F* such that the penalty fee is equal to F times the original real-time price [15], [25].

The aim of the aggregator in the real-time market is to minimize additional cost caused by load mismatch, which is achieved by adjusting EV charging and ES charging/discharging according to the purchased energy from the electricity market one day ahead. Note that since the charging period may span two days, for the first half of the charging period (say, from 12 P.M. to the end of the current day), the aggregator uses the energy usage estimated in the previous day as input for making charging scheduling decisions; while for the second half (say, from midnight to 12 P.M. of the next day), the aggregator uses the energy usage estimated in the current day (before 10 A.M.) as input.

B. Charging Scheduling Model

EVs are connected to the power grid through outlets, which are located in a residence or a charging station. An aggregator serves as a central control node which collects information from both the power grid and connected EVs, and instructs the grid to charge each EV with a charging rate given by a charging scheduling algorithm in each hour. The communications between an aggregator, EVs, and the power grid will be discussed in Section V. The efficient and safe power delivery requires that at any time, the total load does not exceed a *power delivery capacity*, which depends on the physical constraints of power system hardware. In addition, besides energy consumed by EVs, there are basic daily power load contributed by all other electronic appliances (e.g., refrigerators, coffee makers, washing machines, etc), which are referred to as *base load* and should be counted towards the total power load along with the load contributed by EV charging.

An EV can be connected to or disconnected from the power grid at any time according to the user's need. A user inputs the desired finishing time and final SOC of the battery for his car when it is connected to the network. After receiving the information, the aggregator assigns a *charging task* for each EV. Each charging task can be characterized by a 5-tuple (i, s_i, f_i, b'_i, b_i), where i is the vehicle ID, s_i is the starting time, f_i is the desired finishing time, b'_i is the initial SOC of the battery and b_i is the desired SOC after charging. For example, suppose that an EV i is connected to the grid at 6:15 P.M. with an initial SOC of 0.4. It is scheduled to leave at 7:30 A.M. in the next day, with its battery fully charged. Then the corresponding charging task can be presented as $(i, 6.25, 19.5, 0.4, 1)$. There is a one-to-one correspondence between a charging task and an EV and we can use i to denote both the EV ID and charging task ID without abusing the notation. If an EV is charged multiple times during a charging period, it can be assigned a new ID every time it is connected to the charging network.

The aggregator is able to control charging rate of EVs and determine the regulation capacity offered to the grid while performing charging services. We use the unidirectional regulation service model [21] to calculate the regulation capacities. The potential regulation capacity that can be provided by each EV is limited by the operational range of charging rates. The difference between the upper charging rate limit or the maximum charging rate limit (whichever is smaller) and the scheduled charging rate is the regulation-down capacity. The upper charging rate limit P_i is given by the battery of EV, which is the largest rate the battery can draw power at. The maximum charging rate limit is the power needed to charge an EV to its desired SOC in one timeslot, which can be calculated using (8):

$$\bar{P}_{i,t} = \frac{(b_i - x_{i,t}) \times C_i}{E_i}, \quad \forall i, t; \qquad (8)$$

where b_i is the desired SOC of EV i, $x_{i,t}$ is the SOC of EV i at the beginning of timeslot t, C_i is the battery capacity and E_i is the battery charging efficiency of EV i (the ratio between the effectively stored energy and input energy). In addition, when charging a group of EVs, the total regulation-down capacity should be further restricted by the power delivery capacity. Specifically, the aggregator determines the charging rate $p_{i,t}$ for each connected EV to make sure that in each timeslot t, the total charging rate plus the regulation-down capacity is within its upper operational limit, i.e., $\sum_i p_{i,t} + \sum_i d_{i,t} \leq R$, where $d_{i,t}$ is the regulation-down capacity, and R is the power delivery capacity. If ES participate in the charging control, the constraint will be $\sum_i p_{i,t} + \sum_i d_{i,t} + p_{e,t} \leq R$, where $p_{e,t}$ is the charging rate of ES at timeslot t.

The regulation-up capacity is given by the difference between the lower charging rate and the scheduled charging rate of the EV. The regulation capacity is the sum of the regulation-up capacity and the regulation-down capacity: $r_{i,t} = u_{i,t} + d_{i,t}$, based on which the aggregator will be paid by the power grid operator. We calculate the aggregator's revenue, following the model in [22]. The aggregator buys electricity from the market and then

adds a mark-up price M to sell electricity to the EV users for charging their vehicles. On one hand, an aggregator gains income for retailing electricity. On the other hand, an aggregator is paid by the power grid operator for its regulation service. Equation (9) is used to calculate the aggregator's revenue obtained from an EV i in a timeslot:

$$m_{i,t} = a_t r_{i,t} + M e_{i,t}. \tag{9}$$

where $m_{i,t}$ is the revenue from EV i at timeslot t, a_t is the regulation price at timeslot t; $r_{i,t}$ is the regulation capacity from EV i at timeslot t; The total revenue of the aggregator at timeslot t is:

$$m_t = a_t \sum_{i=1}^{N} r_{i,t} + M \sum_{i=1}^{N} e_{i,t}. \tag{10}$$

C. Energy Storage Model

Different types of ES have been studied in power systems for load balancing, ancillary services, etc [15], [23], [26]. All of them have some common characteristics such as high ramping rate, controllable but constrained charging/discharging rate, etc. We consider a general ES model, in which the SOC of ES are bounded by its upper and lower limits [Constraints (11)]. Power loss during discharging and charging operations are captured by the charging efficiency E_e, which is the ratio between the effectively stored energy and input energy. The SOC of ES at the end of an timeslot depends on the SOC in the beginning of the timeslot and the charging rate at that timeslot. For convenience, we split the charging rate of ES $p_{e,t}$ into two variables $p_{c,t}$ (charging) and $p_{d,t}$ (discharging). The ES should either be in the charging state, discharging state or idle state. All constraints related to ES charging/discharging are summarized as follows. The meanings of related notations can be found in the beginning of the paper.

$$\begin{cases} p_{e,t} = p_{c,t} + p_{d,t}; \\ x_{e,t+1} = x_{e,t} + \frac{p_{c,t} E_e}{C_e} + \frac{p_{d,t}}{C_e}; \\ x_{e,0} = b; \\ x_{e,T} \geq b; \\ X' \leq x_{e,t} \leq X; \\ p_{e,t} \in [-P_d, -P'_d] \cup [P'_c, P_c] \cup \{0\}. \end{cases} \tag{11}$$

The aggregator can utilize multiple ES units all together. The total charging/discharging rate limits P_c, P_d and capacity C_e are U times those of a single unit, where U is the number of ES units.

IV. OPTIMIZED CHARGING SCHEDULING

During the charging period, at the beginning of each hour, the aggregator updates the charging schedule for each connected EV, utilizing the real-time price and base load information, and energy usage estimation of the previous day. Since charging an EV usually takes multiple hours but the aggregator can only obtain the real-time information of the current hour, which includes the price (a_t^{real}, g_t^{real}), base load information (l_t^{real}) from the grid and the charging demands for connected EVs.

The price and base load information for the successive hours are estimated using day-ahead forecast data (a_t^{dah}, g_t^{dah} and l_t^{dah}) [17]. Our approach repeatedly calculates the charging rate for each connected EV at the beginning of each hour until the last charging task is fulfilled or the charging period ends. We present the following MILP model for the *Real-time Charging Scheduling with ES Problem (RT-CSP-ES)* at timeslot $t(t \leq T)$:

Unknown Decision Variables:
- $p_{i,t+\tau} \geq 0$: The charging rate of EV i at timeslot $t + \tau$;
- $u_{i,t+\tau} \geq 0$: The regulation-up capacity of EV i at timeslot $t + \tau$;
- $d_{i,t+\tau} \geq 0$: The regulation-down capacity of EV i at timeslot $t + \tau$;
- $z_{c,t+\tau} = \{0, 1\}$: The state of charging of ES, 1 if charging, 0 otherwise;
- $z_{d,t+\tau} = \{0, 1\}$: The state of discharging of ES, 1 if discharging, 0 otherwise;
- $p_{c,t+\tau} \geq 0$: The charging rate of ES if ES is charging;
- $p_{d,t+\tau} \leq 0$: The discharging rate of ES if ES is discharging.

RT-CSP-ES (t)

$$\max_{p_{i,t+\tau}, u_{i,t+\tau}, d_{i,t+\tau}, p_{c,t+\tau}, p_{d,t+\tau} \tau = 0, \dots T-t}$$

$$M \sum_{i=1}^{N} e_{i,t} + M \sum_{\tau=1}^{T-t} \sum_{i=1}^{N} e_{i,t+\tau}$$

$$- \hat{a}_{t,1}^{real} \left(u_t^{est} - \sum_{i=1}^{N} u_{i,t} \right)$$

$$- \sum_{\tau=1}^{T-t} \left(\hat{a}_{t+\tau,1}^{dah} \left(u_{t+\tau}^{est} - \sum_{i=1}^{N} u_{i,t+\tau} \right) \right)$$

$$- \hat{a}_{t,2}^{real} \left(d_t^{est} - \sum_{i=1}^{N} d_{i,t} \right)$$

$$- \sum_{\tau=1}^{T-t} \left(\hat{a}_{t+\tau,2}^{dah} \left(d_{t+\tau}^{est} - \sum_{i=1}^{N} d_{i,t+\tau} \right) \right)$$

$$- \hat{g}_t^{real} \left(\sum_{i=1}^{N} e_{i,t} - e_t^{est} + p_{c,t} + p_{d,t} \right)$$

$$- \sum_{\tau=1}^{T-t} \left(\hat{g}_{t+\tau}^{dah} \left(\sum_{i=1}^{N} e_{i,t+\tau} - e_{t+\tau}^{est} + p_{c,t+\tau} + p_{d,t+\tau} \right) \right). \tag{12}$$

Subject to:

$$x_{i,t+\tau} = \begin{cases} b'_i, & \forall i, t + \tau = \lfloor s_i \rfloor; \\ b_i, & \forall i, t + \tau = \lceil f_i \rceil; \\ x_{i,t+\tau-1} + \frac{E_i e_{i,t+\tau-1}}{C_i}, & \text{otherwise}; \end{cases} \tag{13}$$

$$P_i \geq p_{i,t+\tau} \geq P'_i, \forall i, \tau; \tag{14}$$

$$u_{i,t+\tau} = \begin{cases} p_{i,t+\tau} - P'_i, & \forall i, \tau, s.t. h_{i,t+\tau} = 1; \\ 0, & \text{otherwise}; \end{cases} \tag{15}$$

$$d_{i,t+\tau} = \begin{cases} \min\{\bar{P}_{i,t+\tau}, P_i\} - p_{i,t+\tau}, & \forall i, \tau, s.t. h_{i,t+\tau} = 1; \\ 0, & \text{otherwise}; \end{cases} \tag{16}$$

$$\sum_i^N p_{i,t} + l_t + \sum_i^N d_{i,t} + p_{c,t} + p_{d,t} \leq R; \qquad (17)$$

$$\sum_i^N p_{i,t+\tau} + l_{t+\tau}^{dah} + \sum_i^N d_{i,t+\tau} + p_{c,t+\tau} + p_{d,t+\tau} \leq R,$$
$$\forall \tau \in \{1, \ldots, T-t\}; \qquad (18)$$

$$x_{e,t+\tau} \begin{cases} = b, & \text{if } t+\tau = 0; \\ \geq b, & \text{if } t+\tau = T; \\ = x_{e,t+\tau-1} + \frac{p_{c,t+\tau-1} E_e}{C_e} + \frac{p_{d,t+\tau-1}}{C_e}, & \text{otherwise}; \end{cases} \qquad (19)$$

$$X' \leq x_{e,t+\tau} \leq X, \forall \tau; \qquad (20)$$

$$z_{c,t+\tau} + z_{d,t+\tau} \leq 1; \qquad (21)$$

$$\begin{cases} p_{c,t+\tau} - P_c' z_{c,t+\tau} \geq 0; \\ p_{c,t+\tau} - P_c z_{c,t+\tau} \leq 0; \\ P_d + P_d z_{d,t+\tau} \geq 0; \\ p_{d,t+\tau} + P_d' z_{d,t+\tau} \leq 0. \end{cases} \qquad (22)$$

The RT-CSP-ES (t) actually schedules EV charging for the period between current timeslot t and the end of charging period T. In the problem formulation, the values of the following parameters are given as input: power delivery capacity R; initial/desired SOC b_i'/b_i, starting time s_i, finishing time f_i, and battery capacity C_i of EV i; battery charging efficiency E_i of EV i; the upper and lower charging rate limits P_i and P_i'; the capacity of the ES C_e; the upper and lower charging limits of the ES P_c and P_c'; the upper and lower discharging limits of the ES P_d and P_d'; initial SOC b and the number of ES units U; the charging efficiency of the ES E_e; the mark-up price M; the number of connected EV at timeslot t, N; the day-ahead forecast electricity and regulation service prices at timeslot $(t+\tau)$, $\hat{g}_{t+\tau}^{dah}$ and $a_{t+\tau}^{\hat{d}ah}$, the day-ahead forecast base load at timeslot $(t+\tau)$, $l_{t+\tau}^{dah}$ (where $1 \leq \tau \leq T$); the real-time electricity and regulation service prices at timeslot t, $\hat{g}_t^{real}$, $a_{t,1}^{real}$ and $\hat{a}_{t,2}^{real}$; the real-time base load at timeslot t, l_t^{real}; the estimated hourly energy usage e_t^{est}, the estimated hourly regulation-up capacity u_t^{est} and the estimated hourly regulation-down capacity d_t^{est}.

Eqaution (13) assign a value for the SOC of each connected EV in each hour properly. In this way, each EV is guaranteed to be charged to the desired SOC when it is disconnected from the charging network. In (13), $e_{i,t+\tau}$ gives the energy usage of EV i in timeslot $t+\tau$, which is computed by:

$$e_{i,t+\tau} = h_{i,t+\tau} p_{i,t+\tau}, \forall i, \tau; \qquad (23)$$

where $h_{i,t+\tau}$ gives the actual connection time of each EV during each timeslot. An EV may not always arrive at the beginning of a timeslot and leave at the end of a timeslot. Therefore, the connection time of an EV in a timeslot may be less than one hour and this would affect the calculation of regulation capacities, charging energy, and cost. Note that $h_{i,t+\tau}$ is NOT a decision variable and its value can be pre-calculated using (24) once a charging task is given.

$$h_{i,t+\tau} = \begin{cases} 1, & \lfloor s_i \rfloor < t+\tau < \lfloor f_i \rfloor; \\ 1, & t+\tau = \lfloor s_i \rfloor, s_i = \lfloor s_i \rfloor; \\ \lceil s_i \rceil - s_i & t+\tau = \lfloor s_i \rfloor, s_i \neq \lfloor s_i \rfloor; \\ f_i - \lfloor f_i \rfloor, & t+\tau = \lfloor f_i \rfloor, f_i \neq \lfloor f_i \rfloor; \\ 0, & \text{otherwise}. \end{cases} \qquad (24)$$

Constraints (14) ensure that in each timeslot, the charging rate of each EV is no smaller than its lower limit but no larger than its upper limit. Constraints (15)–(16) calculate the regulation capacities and ensure that for each EV i, the regulation capacity will NOT be accounted in its first and last timeslots (if it does not arrive right at the beginning of its first timeslot or leave at the end of its last timeslot). Constraints (17) and (18) make sure that there is no violation on the power delivery capacity in the current timeslot and in all the successive timeslots respectively. Constraints (19) and (20) assign the value for SOC of ES in each timeslot properly. In this way, at the end of charging period, the SOC of ES is guaranteed to be no less than its initial value. Constraints (21) and (22) ensure that $p_{e,t+\tau} \in [-P_d, -P_d'] \cup [P_c', P_c] \cup \{0\}$, i.e., the charging/discharging rate of ES falls in the allowable range.

The objective (12) of this formulation is to maximize the aggregator's revenue. In the objective function, the values of the real-time balancing price $\hat{g}_t^{real}$, and the real-time balancing regulation-up and regulation-down prices $\hat{a}_{t,1}^{real}$ and $\hat{a}_{t,2}^{real}$ can be calculated using (3), (6), and (7). The values of the day-ahead counterparts $\hat{g}_{t+\tau}^{dah}$, $\hat{a}_{t+\tau,1}^{dah}$ and $\hat{a}_{t+\tau,2}^{dah}$ can be calculated in a similar way using the day-ahead forecast data for all the successive hours ($\tau = 1, \ldots, T-t$) by (25)–(27):

$$\hat{g}_{t+\tau}^{dah} = \begin{cases} (1+F)g_{t+\tau}^{dah}, & \text{if } \sum_{i=1}^{i=N} e_{i,t+\tau} - e_{t+\tau}^{est} + p_{e,t+\tau} > 0; \\ (1-F)g_{t+\tau}^{dah}, & \text{otherwise}; \end{cases} \qquad (25)$$

$$\hat{a}_{t+\tau,1}^{dah} = \begin{cases} (1+F)a_{t+\tau}^{dah}, & \text{if } \sum_{i=1}^{N} u_{i,t+\tau} - u_{t+\tau}^{est} < 0; \\ 0, & \text{otherwise}; \end{cases} \qquad (26)$$

$$\hat{a}_{t+\tau,2}^{dah} = \begin{cases} (1+F)a_{t+\tau}^{dah}, & \text{if } \sum_{i=1}^{N} d_{i,t+\tau} - d_{t+\tau}^{est} < 0; \\ 0, & \text{otherwise}. \end{cases} \qquad (27)$$

$e_{t+\tau}^{est}$, $u_{t+\tau}^{est}$ and $d_{t+\tau}^{est}$ are all given during the real-time operation, which are the estimated energy usage and estimated regulation capacities submitted by the aggregator and accepted by the day-ahead electricity market. The values of those variables can be obtained by solving the MILP model presented above based on day-ahead forecast data in advance.

It is known that solving an MILP may take exponentially long time, especially for large instances [24]. Even though RT-CSP-ES (t) is a complicated MILP problem, it only includes two sets of integer variables $z_{c,t}$ and $z_{d,t}$. So we propose a simple heuristic algorithm based on LP rounding to solve this problem in polynomial time, which is formally presented as Algorithm 1.

Algorithm 1 The LP Rounding Algorithm

Step 1: $\mathcal{P} := \{p_{e,t}, \ldots, p_{e,t+\tau}, \ldots, p_{e,T}\}$;

$\mathcal{Z} := \{z_{e,t}, \ldots, z_{e,t+\tau}, \ldots, z_{e,T}\}$.

Step 2: Solve the LP relaxation of the MILP RT-CSP-ES (t);

Step 3: **forall** $p_{e,t+\tau} \in [-P_d, -P_d'] \cup [P_c', P_c] \cup \{0\}$

    if $(p_{e,t+\tau} > 0)$, $z_{e,t+\tau} := 1$;

elseif $(p_{e,t+\tau} = 0)$, $z_{e,t+\tau} := 0$;

    else $z_{e,t+\tau} := -1$.

  endif

  endforall

Step 4: **forall** $p_{e,t+\tau} \notin [-P_d, -P'_d] \cup [P'_c, P_c] \cup \{0\}$ Choose τ_m s.t. $\min\{|p_{e,t+\tau_m} - 0|, |p_{e,t+\tau_m} - P'_c|, |p_{e,t+\tau_m} + P'_d|\}$ is minimum among all such values;

  if $(p_{e,t+\tau_m} \geq P'_c/2)$, $z_{e,t+\tau_m} := 1$;

    elseif $(p_{e,t+\tau_m} \leq -P'_d/2)$, $z_{e,t+\tau_m} := -1$;

    else $z_{e,t+\tau_m} := 0$.

  endif

  endforall

Step 5: **if** (The values of variables in $\mathcal{Z}$ and $\mathcal{P}$ are all determined)

    return $\mathcal{P}$ and $\mathcal{Z}$;

    else goto Step 2.

Algorithm 1 rounds integer variables iteratively until the values of all integer variables are determined. In Step 3 of this algorithm, for all the $p_{e,t+\tau}$ such that $p_{e,t+\tau} \in [-P_d, -P'_d] \cup [P'_c, P_c] \cup \{0\}$ (i.e., the value falls in the allowable range), we can determine the corresponding states $z_{e,t+\tau}$: charging (positive), discharging (negative) or idle (0), according to the signs of the values of $p_{e,t+\tau}$. However, for all the $p_{e,t+\tau}$ such that $p_{e,t+\tau} \notin [-P_d, -P'_d] \cup [P'_c, P_c] \cup \{0\}$ (Step 4), we calculate the distances between each value of $p_{e,t+\tau}$ and three boundary values $\{0, P'_c, P'_d\}$ respectively. The one with shortest distance wins and the corresponding state $z_{e,t+\tau_m}$ is determined accordingly. Note that in this case, only one integer variable's value is determined in one step. The LP rounding algorithm is a polynomial time algorithm. It solves T LPs (where T is the number of timeslots), each of which has polynomial numbers of variables and constraints. In practice, we observed it took less than 1 sec for the case with 300 EVs, using a PC with a 2.4 GHz i7–2760 QM CPU and 8 GB RAM.

V. COMMUNICATION PROTOCOL

In order to apply the proposed charging scheduling approach in a real system, the aggregator, the power grid, and EVs need to constantly exchange information. However, it currently lacks a standard for communications between different entities in a smart grid system. We hereby introduce a communication protocol to enable EV charging control.

Bidirectional communications are needed for charging control. Fig. 1 illustrates the information that needs to be exchanged between different entities. Specifically, the aggregator collects the charging demand (i.e., starting time, finishing time, initial SOC, and desired SOC) from each EV, and instructs it to charge with a certain rate computed by a charging scheduling algorithm. Moreover, the aggregator collects the energy availability information from the ES, and instructs it to charge/discharge
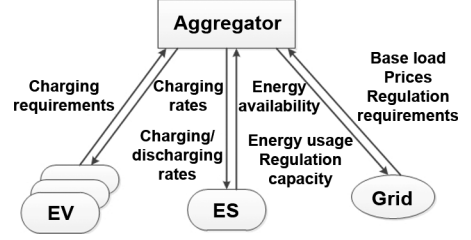

Fig. 1. The information exchanged between different entities.
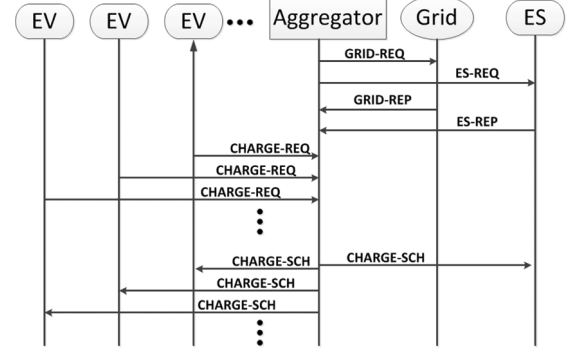

Fig. 2. The message flow between different entities.

with a certain rate computed by a charging scheduling algorithm. In addition, the aggregator is notified by the power grid with its capacity, pricing information, and regulation requirements, and informs the power grid with energy usage and its regulation capacity.

In Fig. 2, we show the message flow in the real-time charging operations. At the beginning of each hour, the aggregator sends a GRID-REQ message to the power grid to request for base load and pricing information. The power grid replies with a Grid-REP message with requested information. Similarly, the aggregator sends an ES-REQ message to the ES for its available energy and the ES replies with an ES-REP message. Every time when an EV is connected to a charger, the charger collects its current SOC and the user's demand information from a user interface, and packs them in a CHARGE-REQ message and sends it to the aggregator. The aggregator runs a charging scheduling algorithm (e.g., Algorithm 1) at the beginning of each hour to determine the charging rates for EVs and the charging/discharging rate for the ES and sends CHARGE-SCH messages to both EVs and the ES such that the corresponding outlets and ES can follow to charge.

VI. SIMULATION RESULTS

We evaluated the performance of the proposed approach using real electricity prices, base load, and EV battery data. Specifically, the hourly electricity prices and regulation prices in each day in the Central New York were obtained from the NYISO [17]. Average electricity prices and regulation prices over 30 days (July 1–July 30, 2011) were used for simulation. We set EV battery related parameters, including the charging rate limit and battery capacity based on the specification of the Volt Li-ion battery of a modern EV model [3]. A typical summer base load profile for a 1000-household residential community was obtained from the demand profile generator of University of Strathclyde [18]. A total of 10 seeds (from 1 to

TABLE I
SIMULATION SETTINGS

Mean of s_i	6 pm
Mean of f_i	7 am
Standard deviation of s_i	2 h
Standard deviation of f_i	2 h
b_i	1
b	0.5
E_i	0.9
C_i	16 kWh
R	2000 kW
T	24
M	$0.05 [22]
P_i	4.4 kW
P_i'	0 kW

TABLE II
ES-RELATED PARAMETERS

Capacity (kWh)	100
Minimum charging rate (kW)	5
Minimum discharging rate (kW)	5
Maximum charging rate (kW)	25
Maximum discharging rate (kW)	25

10) were used to generate 10 sets of random input data and the average values over 10 runs were presented as results in the following figures.

In the simulation for day-ahead energy usage estimation, N charging tasks were generated for a scheduling period from 12 P.M. (noon) to 12 P.M. in the next day to simulate the overnight EV charging. We followed the statistical behavior model in [7] to generate *day-ahead* EV charging demands. The starting time s_i followed a normal distribution with a mean of $\mu = 6$ P.M. and a standard deviation of $\sigma = 2$ hours; the desired finishing time f_i followed a normal distribution with $\mu = 7$ A.M. and $\sigma = 2$ hours; and the initial SOC b_i' was also a random variable uniformly distributed in the range $[0, 1]$. The desired SOC was set to 1 (fully charged) for each EV, i.e., $b_i = 1, i \in \{1, \ldots, N\}$. For the sake of battery health, the ES charging state can only be changed in the beginning of an hour. The initial SOC of ES was set to 0.5. The related simulation settings are summarized in Table I. The values of key parameters of a single ES unit are given in Table II ([23]):

In the simulation, an unregulated charging scheme was used as a baseline method for comparison, in which the aggregator serves EVs on a first come first serve basis and charges EVs with the maximal allowable charging rate, and no regulation service is provided. We used the aggregator's revenue as the performance metric. The following parameters may have a significant impact on system performance: the number of EVs (N), the number of ES units (U), the penalty factor (F) and the mismatch between the predicted finishing time and the actual value. We designed different scenarios to test their impacts. We first computed the day-ahead (static) charging schedules using the MILP model presented above based on predicted 48-hour charging demands. Both regulated and unregulated day-ahead charging schedules (DAH-Regulated and DAH-Unregulated) were calculated and the corresponding hourly energy usages will be used as estimated energy usage values for real-time charging scheduling. Moreover, the revenues given by the DAH schemes can be used as benchmarks for performance
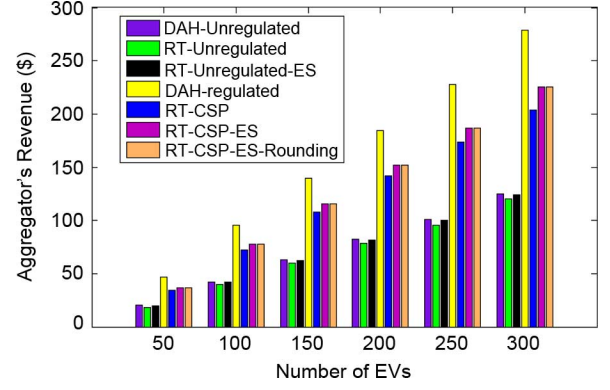

Fig. 3. The revenues vs. the number of EVs N.

comparison with real-time scheduling. For real-time charging scheduling, four schemes were simulated: the real-time unregulated charging scheduling without ES (RT-Unregulated), the real-time optimal charging scheduling without ES (RT-CSP) and the real-time unregulated charging scheduling with ES (RT-Unregulated-ES), and the real-time optimized charging scheduling with ES. For the last scheme, we obtained the optimal charging schedules by solving the corresponding MILP problem using the Gurobi Optimizer [8] (RT-CSP-ES) and the suboptimal solutions using the LP rounding algorithm (RT-CSP-ES-Rounding).

A. Revenue Gains Given by Optimized Charging Scheduling

To show the revenue gains that can be brought by optimal charging scheduling, we compared our optimal charging scheduling schemes with the baseline method. In the simulation, we fixed the penalty factor at 0.5, the number of ES units at 15 and the mean real-time finishing time at 4 A.M.. Moreover, we performed simulation runs on systems with $N = \{50, 100, 150, 200, 250, 300\}$. The results are shown in Fig. 3.

From Fig. 3 we can make three important observations: 1) Significant revenue gains can be brought by optimized charging scheduling. Specifically, on average, without using ES, optimal charging scheduling improves the aggregator's revenue by 80.1%, compared to unregulated charging. 2) When ES is utilized for load matching, a further increase of 7.8% in revenue is achieved. 3) The aggregator's revenues given by the LP rounding algorithm are almost always the same as the optimal values. The average difference is less than 0.1%. Therefore, we conclude that the LP rounding algorithm can provide close-to-optimal solutions in polynomial time.

B. Benefits Given by Utilizing ES for Load Matching

To show the load matching benefits that can be brought by real-time charging scheduling utilizing ES while the day-ahead EV distribution prediction is not accurate, we show the reduction in load mismatch on cases with different numbers of ES units and compare the revenue obtained by the RT-CSP-ES scheme with the revenue obtained by the RT-CSP scheme (without aid of ES). In the simulation, we performed simulation runs on EV groups with a size of $N = 300$. The mean real-time finishing time were set to 4 A.M., and a penalty factor $F = 0.5$.
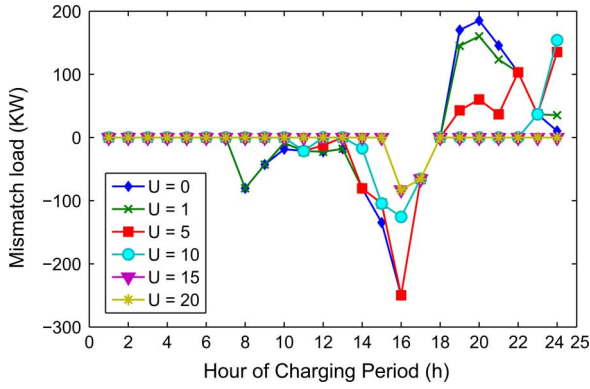
Fig. 4. The load matching effect given by optimal charging scheduling with different numbers of ES units.
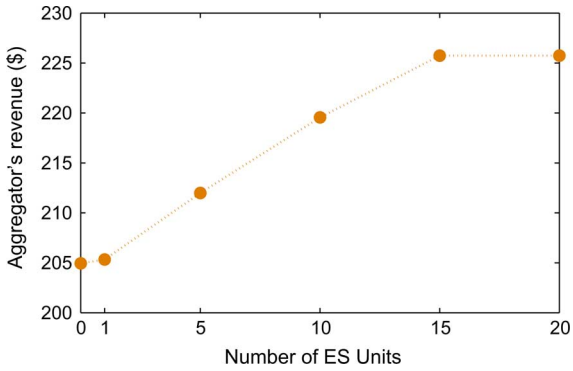

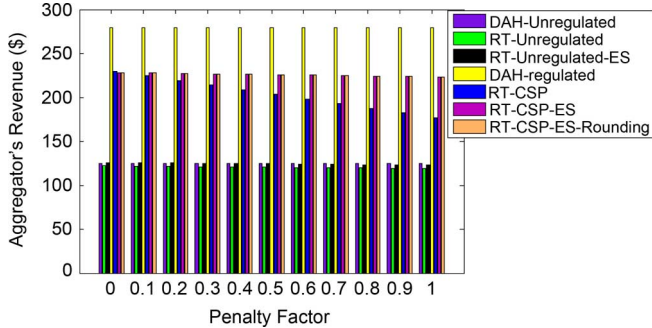Fig. 5. The revenues given by optimal charging scheduling with different numbers of ES units U.

Fig. 6. The revenues vs. the penalty factors F.

The number of ES units were set to $U = \{0, 1, 5, 10, 15, 20\}$. The results are shown in Figs. 4 and 5.

From Fig. 4, we can clearly see that as the number of ES units increases, the mismatch between day-ahead energy usage estimation and real-time energy usage is mitigated, and consequently, the aggregator's revenue increases (Fig. 5). However, as the number of ES units increases to more than 15, the load mismatch cannot be further mitigated since all the load mismatches now are negative (i.e., the actual energy usage is more than the estimated energy usage) and the revenue saturates.

C. Impact of Penalty Factor on the Aggregator's Revenue

In the electricity market, the penalty factor may fluctuate over time. We performed simulation runs on EV groups with a size of $N = 300$ and with $U = 15$. The penalty factor F increases from 0 to 1, with a step size of 0.1. The results are shown in Fig. 6.
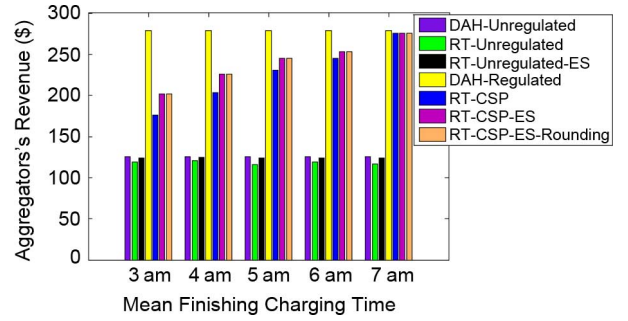

Fig. 7. The revenues vs. the mean finishing times.

From the results, we can see that the penalty factor has a greater impact on optimized (regulated) charging schemes than unregulated schemes. The aggregator needs to take that into consideration when determining whether or not to participate in regulation. However, as Fig. 6 shows, when ES is utilized, with F increases, the average revenue gain brought by optimal charging scheduling is still significant, around 82% (compared to unregulated charging); without ES, the average revenue gain drops to 68%.

D. Impact of Inaccurate Finishing Time Prediction on the Aggregator's Revenue

In real time, the actual charging demands might be different from the estimated values. We want to investigate the impact of inaccurate prediction on the aggregator's revenue. We used the finishing time as a representative parameter to illustrate such an impact. In this scenario, the (day-ahead) estimated mean finishing time was set to 7 A.M. (of the next day). For real-time scheduling, we set mean finishing time to $\{3, 4, 5, 6, 7\}$ A.M. instead. In addition, $N = 300$, $U = 15$, and $F = 0.5$. The corresponding results are shown in Fig. 7.

From the results, we can see the inaccurate estimation of mean finishing time does not have a great impact on unregulated schemes; however, for optimized charging scheduling schemes, the impact is greater. This is because, optimized charging scheduling leads to a more even distribution of charging loads while the unregulated method is a greedy approach which draws more energy during the early part of the charging period. As the mean finishing time deviates more from the predicted values, the reduction on the aggregator's revenue is more significant. Specifically, when the mean finishing charging time is 4 hours earlier than the predicted values (i.e., 3 A.M.), on average, the reduction in revenue for the optimal (regulated) charging scheduling scheme is 36.8% (compared to the values corresponding to accurate prediction, i.e., 7 A.M.) when no ES is used and 27.6% when ES is used.

VII. CONCLUSION

In this paper, we studied an optimization problem of scheduling EV charging with ES with joint consideration for the day-ahead and real-time markets. We presented an MILP model to provide optimal solutions as well as an LP rounding based heuristic algorithm to solve the problem in polynomial time. In addition, we also presented a communication protocol for interactions among different entities including the aggregator, the power grid, the ES, and EVs. It has been shown by extensive

simulation results based on real electricity price and load data that compared to a baseline method without charging regulation, the aggregator's revenue can be improved by 80.1% using optimal charging scheduling and can be further improved by 7.8% with the aid of ES on average. The proposed heuristic algorithm yields close-to-optimal solutions. Moreover, we investigated how several key parameters (including the number of EVs, the number of ES units, the penalty factor, and the prediction accuracy) affect the performance of the proposed approach.

REFERENCES

[1] P. H. Andersen, J. A. Mathews, and M. Raska, "Integrating private transport into renewable energy policy: The strategy of creating intelligent recharging grids for electric vehicles," *Energy Policy*, vol. 37, no. 7, pp. 2481–2486, 2009.

[2] R. J. Bessa *et al.*, "Optimized bidding of an EV aggregation agent in the electricity market," *IEEE Trans. Smart Grid*, vol. 3, no. 2, pp. 443–452, 2012.

[3] Chevy Volt Specifications [Online]. Available: http://www.chevrolet.com/volt/.

[4] M. S. Bazaraa, J. J. Jarvis, and H. D. Sherali, *Linear Programming and Network Flows*, 3rd ed.   Hoboken, NJ: Wiley, 2005.

[5] K. Clement, E. Haesen, and J. Driesen, "The impact of charging plug-in hybrid electric vehicles on a residential distribution grid," *IEEE Trans. Power Syst.*, vol. 25, no. 1, pp. 371–380, 2010.

[6] D. Dallinger, D. Krampe, and M. Wietschel, "Vehicle-to-grid regulation reserves based on a dynamic simulation of mobility behavior," *IEEE Trans. Smart Grid*, vol. 2, no. 2, pp. 302–313, 2011.

[7] "Summary of travel trends, 2009 National Household Travel Survey," U.S. Department of Transportation, 2009.

[8] Gurobi [Online]. Available: http://www.gurobi.com/.

[9] S. Han, S. Han, and K. Sezaki, "Development of an optimal vehicle-to-Grid aggregator for frequency regulation," *IEEE Trans. Smart Grid*, vol. 1, no. 1, pp. 65–72, 2011.

[10] S. Jang *et al.*, "Optimal decision on contract size for V2G aggregator regarding frequency regulation," in *Proc. Int. Conf. Optim. Elect. Electron. Equipment*, 2010, pp. 54–62.

[11] M. G. Kallitsis, G. Michailidis, and M. Devetsikiotis, "A decentralized algorithm for optimal resource allocation in smartgrids with communication network externalities," in *Proc. IEEE Smart Grid Commun.*, 2011, pp. 434–439.

[12] W. Kempton and J. Tomic, "Vehicle-to-grid power implementation: From stabilizing the grid to supporting large-scale renewable energy," *J. Power Sources*, vol. 144, no. 1, pp. 280–294, 2005.

[13] W. Kempton *et al., A Test of Vehicle-to-Grid (V2G) for Energy Storage and Frequency Regulation in the PJM System*.   Newark, DE: Univ. Delaware, 2008.

[14] W. Kempton and J. Tomic, "Vehicle-to-grid power fundamentals: Calculating capacity and net revenue," *J. Power Sources*, vol. 144, no. 1, pp. 268–279, 2005.

[15] M. Korpas and A. T. Holen, "Operation planning of hydrogen storage connected to wind power operating in a power market," *IEEE Trans. Energy Convers.*, vol. 21, no. 3, pp. 742–749, 2006.

[16] P. Kulshrestha *et al.*, "Evaluation of ZigBee communication platform for controlling the charging of PHEVs at a municipal parking deck," in *Proc. IEEE Veh. Power Propulsion Conf.*, 2009, pp. 1211–1214.

[17] Whole-Sale Power, NYISO [Online]. Available: http://www.eia.gov/cneaf/electricity/wholesale/new_yorkiso.html.

[18] Demand Profile Generators [Online]. Available: http://www.strath.ac.uk/esru/.

[19] C. Quinn, D. Zimmerle, and T. H. Bradley, "The effect of communication architecture on the availability, reliability, and economics of plug-in hybrid electric vehicle-to-grid ancillary services," *J. Power Sources*, vol. 195, no. 5, pp. 1500–1509, 2010.

[20] C. Sandels, U. Franke, and L. Nordström, "Vehicle to grid communication monte carlo simulations based on automated meter reading reliability," in *Proc. Power Syst. Comput. Conf.*, 2011.

[21] E. Sortomme *et al.*, "Coordinated charging of plug-in hybrid electric vehicles to minimize distribution system losses," *IEEE Trans. Smart Grid*, vol. 2, no. 1, pp. 198–205, 2011.

[22] E. Sortomme and M. A. El-Sharkawi, "Optimal charging strategies for unidirectional vehicle-to-grid," *IEEE Trans. Smart Grid*, vol. 2, no. 1, pp. 131–138, 2011.

[23] R. Walawalkara, J. Apta, and R. Mancini, "Economics of electric energy storage for energy arbitrage and regulation in New York," *Energy Policy*, vol. 35, no. 4, pp. 2558–2568, 2007.

[24] L. A. Wolsey, *Integer Programming*.   New York: Wiley, 1998.

[25] Y. Xu, L. Xie, and C. Singh, "Optimal scheduling and operation of load aggregator with electric energy storage in power markets," in *Proc. North Amer. Power Symp.*, 2010.

[26] Y. Xu, L. Xie, and C. Singh, "Optimal scheduling and operation of load aggregators with electric energy storage facing price and demand uncertainties," in *Proc. North Amer. Power Symp.*, 2011.

[27] H. Zhang and M. Chow, "Comprehensive dynamic battery modeling for phev applications," in *Proc. IEEE Power Energy Soc. Gen. Meet.*, 2010, pp. 25–29.

Chenrui Jin (S'09) earned her B.S. degree in physics and mathematics from Tsinghua University, Beijing, China, in 2007 and M.S.E.E. degree from Syracuse University, Syracuse, NY, in 2010. She is working toward the Ph.D degree in the Department of Electrical Engineering and Computer Science at Syracuse University.

Her research interests include power system optimization, vehicle to grid technologies, distributed energy sources, and energy management system.

Jian Tang received his Ph.D. degree in Computer Science from Arizona State University, Tempe, in 2006.

He is an Assistant Professor in the Department of Electrical Engineering and Computer Science at Syracuse University, Syracuse, NY. His research interests lie in the areas of wireless networking, cloud computing, and green networking.

Dr. Tang received an NSF CAREER Award in 2009. He served as a symposium co-chair for the IEEE Globecom'2011 Wireless Networking Symposium and the ICNC'2012 Wireless Networks Symposium. He has also served on the technical program committees of many international conferences such as IEEE Infocom, ICC, Globecom, and so on.

Prasanta Ghosh is a Professor in the Department of Electrical Engineering and Computer Science at Syracuse University, Syracuse, NY. He conducts research in the area of microelectronics and power engineering. As a Fulbright Scholar he has traveled internationally to teach engineering students and delivered lectures on his research. His current research work includes smart grid, design and analysis of nanodevices, and thin film gas sensors.